# Interfacial Tension Errors from the Cohen and Carriere Analysis of Imbedded Fiber Retraction

**J. Martin and S. Velankar***

*Department of Chemical Engineering, University of Pittsburgh, Pittsburgh, Pennsylvania 15261*

*Received March 9, 2005*
*Revised Manuscript Received September 29, 2005*

## 1. Introduction

Immiscible polymers are often blended together to create new materials with desired properties. Knowledge of the interfacial tension between the immiscible polymers is important when designing such blending processes. Traditional methods of measuring the interfacial tension between low molecular weight fluids, e.g., the pendant or sessile drop method, the Wilhelmy balance, and the spinning drop method, do not work well for molten polymers because their high viscosity requires unacceptably long times for equilibration. Therefore, "dynamic" methods, which use the kinetics of interfacial tension-driven motion to obtain the interfacial tension, have been devised for polymers.[1−6] One such method, the imbedded fiber retraction method, is the subject of this paper. The purpose is to demonstrate that the Cohen and Carriere (CC) model[1,2] that is commonly used to analyze fiber retraction experiments can cause large errors in interfacial tension, whereas an alternate analysis by Tjahjadi, Ottino, and Stone (TOS)[7] gives reliable interfacial tension values. A notable feature of our experimental approach is that the fiber retraction experiments are benchmarked rigorously: we are able to measure the *equilibrium* interfacial tension *in the same experiment* as the fiber retraction.

## 2. Theory

The fiber retraction experiment consists of imbedding an approximately cylindrical fiber of one polymer in a matrix of the other, and then melting the system to allow interfacial tension to change the shape of the fiber. Regardless of the details of initial fiber shape, the fiber rapidly takes on an approximately spherocylindrical (cylinder with hemispherical end-caps) shape. Subsequent shape evolution is imaged periodically. The fiber retracts toward a spherical shape at a rate that is determined by the interfacial tension driving the retraction, and the viscous resistance to the retraction. The principle of the fiber retraction method is to obtain the interfacial tension by fitting a theoretical model of the retraction to the experimental retraction kinetics. While polymers are generally viscoelastic, due to the very low interfacial stress driving retraction, it is generally reasonable to assume that the fiber and the matrix behave as Netwonian fluids.

Even with the assumption of Netwonian behavior, however, the retraction of a cylindrical fiber is quite complex:[8] the shape can evolve from an initial cylinder into a "dumbbell" with bulbous ends, followed by an ellipsoid, and finally a sphere (see Figure 1a). Therefore, models of retraction do not predict the details of the shape of the fiber, but instead only predict the time-evolution of some convenient geometrical features of the shape. These features are shown in Figure 1b. The first is the overall length of the fiber, denoted as $2L$. The second is the effective diameter, $2a$, of a spherocylinder with the same volume as the fiber. The last is the radius, $R_0$, of the sphere finally resulting at the end of retraction. Obviously

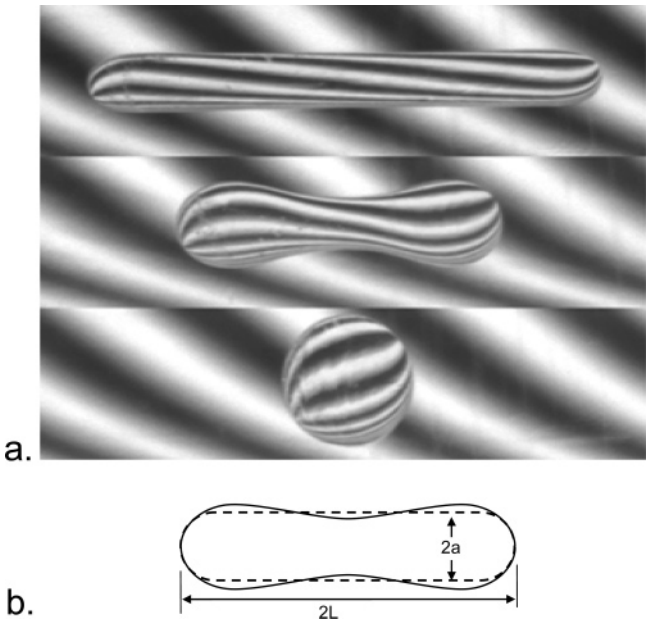


**Figure 1.** (a) Shapes of a drop with $p = 0.368$ during retraction. The alternating black and white stripe pattern in the background helps define the edge of the drop clearly even if the refractive index difference of the fiber is close to that of the matrix. (b) Geometric parameters for analysis: The dotted line a spherocylinder of the same length and volume as the actual drop. The diameter $2a$ is obtained by solving eq 1.

$$\text{volume of fiber} = \frac{4}{3}\pi R_0^{\,3} = 2\left(\pi a^2(L-a) + \frac{2}{3}\pi a^3\right) \quad (1)$$

The initial length and effective radius are denoted as $L_0$ and $a_0$ respectively. Experimentally one may either measure $L(t)$ and $R_0$ (if the fiber retracts all the way up to spherical shape) or $L(t)$ and $a_0$ (if the experiment is stopped before complete retraction). In either case, the fiber volume can be calculated, allowing $a(t)$ to be calculated from $L(t)$.

**Cohen and Carriere Analysis.** Due to the considerable complexity of the retraction process[8] there is no rigorous analytical equation to describe the evolution of $L$ or $a$ with time. Hence Cohen and Carriere, who first proposed the fiber retraction method, developed an approximate model of the retraction kinetics.[1,2] They assumed that the fiber remained spherocylindrical *at all times* and predicted

$$f\left(\frac{a}{R_0}\right) - f\left(\frac{a_0}{R_0}\right) = \frac{t\sigma}{R_0\mu_e} \quad (2)$$

where

10.1021/ma050509k CCC: $30.25 
Published on Web 11/16/2005

$$f(x) = 1.5 \ln\left(\frac{\sqrt{1+x+x^2}}{1-2}\right) + \frac{3^{1.5}}{2} \arctan\left(\frac{x\sqrt{3}}{2+x}\right) - \frac{x}{3} - \frac{4}{x} \quad (3)$$

In eq 2, $\sigma$ is the interfacial tension, $t$ is the time, and $\mu_e$ is the effective viscosity:[1,2]

$$\mu_e = \mu_m \frac{1+1.7p}{2.7} \quad (4)$$

where the viscosity ratio $p = \mu_f/\mu_m$ is the ratio of the fiber viscosity $\mu_f$ to the matrix viscosity $\mu_m$. The effective viscosity is intended to capture the dependence of the retraction kinetics on both the matrix as well as the fiber viscosity.

To apply the CC model, $L(t)$ is measured experimentally, the equivalent radius $a(t)$ is determined by solving eq 1, and $f(a/R_0) - f(a_0/R_0)$ is plotted vs time. Equation 2 suggests that a straight line will be obtained with a slope $\sigma/R_0\mu_e$. The values of $\sigma$ obtained this way are denoted by $\sigma_{CC}$ in this paper.

**Tjahjadi, Ottino, and Stone Analysis.** Recognizing that the CC model is approximate, Tjahjadi et al.[7] subsequently took a more rigorous approach. Assuming only the *initial* shape of the fiber to be a spherocylinder, they integrated the Stokes equations exactly using the boundary integral method to calculate the subsequent shapes during retraction. For experimental convenience, the results of the evolution of $L$ with time were presented as a fourth-order polynomial approximation:

$$\frac{L}{R_0} = \sum_{n=0}^{4} k_n \left(\frac{t\sigma}{\mu_m a_0}\right)^n \quad (5)$$

Dimensional analysis requires that the polynomial coefficients $k_n$ depend on only two dimensionless parameters, the viscosity ratio $p$ and the initial aspect ratio, $L_0/a_0$. Accordingly, $k_n$ were tabulated at several values of $p$ and $L_0/a_0$.[7]

To apply the TOS model, the coefficients $k_n$ at the experimental $p$ and $L_0/a_0$ are first determined by linear interpolation of the tabulated $k_n$. Then the experimental $L/R_0$ is plotted vs time and fitted to eq 5 using $\sigma$ as a fitting parameter. The values of $\sigma$ obtained this way are denoted by $\sigma_{TOS}$ in this paper. The original paper[7] recommended an alternative procedure of fitting eq 5 to the $L/R_0$ of just two images of a retracting drop, taken a known time interval apart. That procedure[7] is more convenient to users who do not have an imaging method, e.g., a camera, since two $L$ values can be measured with just a calibrated microscope. Furthermore, since only two values are used, finding $\sigma$ does not require data-fitting. The procedure used here is much more rigorous since the evolution of $L/R_0$ over a much wider time interval is used for fitting. A limited amount of data-fitting is required but, as mentioned below, even "visual" fits are sufficient and regression is not required.

**Equilibrium Measurements.** Finally, we measured the equilibrium interfacial tension using a spinning drop tensiometer (SDT).[9−11] In this instrument, the higher density fluid is loaded into a glass tube and a drop of the lower density fluid is suspended in it. The tube is spun rapidly about its axis to cause the drop to centrifuge to the center and achieve an elongated, nearly spherocylindrical, shape.[10] This shape is an equilibrium between interfacial and centrifugal forces, and the interfacial tension can be calculated from[9,10]

$$\sigma = \frac{\Delta\rho\omega^2 {a_0}^3}{4} \text{ provided } \frac{L_0}{a_0} > 4 \quad (6)$$

where $a_0$ is the radius of the spherocylindrical drop, $\Delta\rho$ the density difference between the droplet and matrix, and $\omega$ the rotational speed. The values of $\sigma$ obtained this way are denoted by $\sigma_{eq}$ in this paper.

As mentioned at the end of the Introduction, the advantage of using the SDT is that equilibrium interfacial tension can be obtained from the radius of the spherocylindrical drop while spinning, and the retraction recorded immediately afterward by stopping the spinning. Thus, the interfacial tension is measured by both an equilibrium method and a retraction method *independently* in the same experiment, allowing a rigorous test of the CC and the TOS analyses of fiber retraction.

**Table 1. Properties of Materials Used**

| | fluid | density (kg/m$^3$) | $\mu$ (Pa·s) |
|---|---|---|---|
| matrix | PDMS 30 000 | 972 | 33.1 |
| | PDMS 100 000 | 972 | 93.2 |
| drop | PIB 24 | 898 | 34.3 |
| | PIB 32 | 904 | 67.3 |
| | PIB 124 | 904 | 483 |
| | polybutadiene | 900 | 3.08 |

## 3. Experimental Section

**Materials.** Poly(dimethylsiloxane) (PDMS) (Rhodia Silicones) and polyisobutylene (PIB) (Soltex Chemicals) were used as the matrix and drop phases, respectively, for viscosity ratios of 0.368, 0.722, 2.03, and 5.18. For a viscosity ratio of 0.033, PDMS was used as the matrix phase and polybutadiene (Aldrich) as the drop phase. Some properties of the materials used are listed in Table 1. All materials were Newtonian under experimental conditions and their viscosities were measured at room temperature using a TA Instruments AR 2000 rheometer. All polymers were used as received.

**SDT and Calibration.** Experiments were performed at room temperature in a home-built SDT using a precision bore glass tube of inner diameter 12.7 mm. Because of lensing effects of the cylindrical tube, images of drops inside the tube appear distorted, and accurate calibration of the drop dimensions along the axial and the radial direction of the tube is crucial. Calibration was done as follows: In all pairs of fluids, the PDMS is the higher density phase and forms the matrix. Accordingly, each PDMS fluid was loaded into the SDT tube and a solid polyethylene sphere of known diameter was suspended in it and spun. Since polyethylene has a lower density than PDMS, the sphere centered itself along the axis of rotation, and was imaged. In the images, the sphere appeared elliptical, with the ratio of its radial dimension to its axial dimension being roughly 1.4. This ratio, which is close to the refractive index of PDMS as expected,[12] was used to correct the images of drops so as to obtain their dimensions accurately.

**Interfacial Tension Measurements.** The desired PDMS was loaded into the SDT tube, and the desired PIB or PI was added as a drop. The tube was spun at constant speed (typically 3000−9000 rpm) until a steady drop shape of a convenient aspect ratio was reached,

**Table 2. Interfacial Tension in mN/m Calculated for Various Viscosity Ratios and Initial Aspect Ratios**

| system | $p$ | $L_0/a_0$ | $\sigma_{eq}$ [a] | $\sigma_{CC}$ [b] | $\sigma_{TOS}$ [c] |
|---|---|---|---|---|---|
| polybutadiene/PDMS 100 000 | 0.033 | 2.95 | | 3.9 | 5.0 |
| | | 5.13 | 4.9 | 4.9 | 5.0 |
| | | 5.72 | | 4.6 | 4.8 |
| | | 6.42 | | 4.3 | 4.5 |
| | | 7.92 | | 4.4 | 4.5 |
| | | 8.72 | | 4.8 | 4.6 |
| PIB 24/PDMS 100 000 | 0.368 | 3.47 | | 1.9 | 2.1 |
| | | 6.20 | 1.7 | 1.8 | 2.0 |
| | | 9.43 | | 1.6 | 1.8 |
| | | 10.3 | | 1.6 | 1.7 |
| PIB 32/PDMS 100 000 | 0.722 | 4.05 | 2.2 | 3.2 | 2.8 |
| | | 4.95 | | 3.1 | 2.8 |
| | | 8.28 | | 2.8 | 2.7 |
| | | 9.63 | | 2.6 | 2.6 |
| | | 14.1 | | 2.6 | 2.2 |
| PIB 32/PDMS 30 000 | 2.03 | 4.65 | 2.9 | 5.3 | 3.3 |
| | | 8.61 | | 5.5 | 2.9 |
| | | 8.78 | | 7.0 | 3.4 |
| | | 9.72 | | 7.3 | 3.2 |
| PIB 124/PDMS 100 000 | 5.18 | 5.32 | 3.0 | 8.3 | 3.5 |
| | | 5.85 | | 8.7 | 3.5 |
| | | 7.33 | | 9.0 | 3.3 |
| | | 7.98 | | 9.4 | 3.4 |
| | | 8.48 | | 8.9 | 3.3 |

[a] From eq 6; average of spinning drops with $L_0/a_0 > 4$. [b] Least-squares fit of eq 2 to $f(a/R_0) - f(a_0/R_0)$ vs $t$ data. [c] Least-squares fit of eq 5 to $L/R_0$ vs $t$ data.

and the drop was imaged. The rotational speed was then abruptly reduced to a low value (about 500 rpm), and the subsequent retraction was imaged. Rotation could not be ceased altogether because the droplet would rise to the top of the tube due to buoyancy. Limited experiments on drops of different sizes confirm that this slow rotation at 500 rpm does not affect the interfacial tension obtained from the retraction kinetics significantly. This procedure (equilibration at a certain aspect ratio, followed by retraction) was repeated at four or more rotational speeds. In all cases, the diameter of the retracting drop was no more than 20% of the inner diameter of the tube.

The radii, $a_0$, of the drops during steady spinning gave the equilibrium interfacial tensions, $\sigma_{eq}$, from eq 6. These are listed in Table 2. Consistent values were obtained at all rotational speeds giving confidence that equilibrium was indeed reached.

Furthermore, radii, $a_0$, and the lengths, $L_0$, of the drops during steady spinning also gave the drop volumes from eq 1. The images of the drops recorded during retraction gave $L(t)$ directly; these combined with the drop volume gave the effective radius, $a(t)$ of the drops during retraction.

**Error Estimates.** For the equilibrium interfacial tension, the errors can be estimated easily from eq 6. We estimate approximately 4% error in $a_0$, 3% error in $\omega$ and less than 2% error in the density. These result in a cumulative 14% error in the equilibrium interfacial tension.

Errors in the retraction analysis are more difficult to estimate. Because of fluctuations in room temperature, there is some uncertainty (less than 5%) in the viscosity. The 4% error in $a_0$ cited above causes uncertainty in the drop volume (eq 1), and hence in the calculated value of $a(t)$ and of $R_0$. Finally, for the TOS method, uncertainties in the viscosity ratio and in the initial aspect ratio ($L_0/a_0$) cause slight uncertainty in the $k_n$ values (fortunately, the $k_n$ values are not highly sensitive to $p$ or $L_0/a_0$). An approximate sensitivity analysis suggests that the theoretical cumulative error in $\sigma_{CC}$ and $\sigma_{TOS}$ is no more than 15%. Practically, however, application of the CC model can have additional error: $f(a/R_0) - f(a_0/R_0)$ vs time plots are not always linear (see Figure 2) and significant error can result from the arbitrariness in picking the "linear" region for fitting.

## 4. Results and Discussion

Substituting $\sigma = \sigma_{eq}$ into eqs 2 and 5 result in predictions of the retraction kinetics of the CC and the TOS models, respectively. Here we will first compare these predictions to the measured retraction kinetics at all values of $p$, but only for drops with initial aspect ratios close to 8. These will qualitatively illustrate whether the two models are able successfully reproduce the retraction kinetics or not. This is done in Figures 2 and 3, which are discussed further below.

Furthermore, eqs 2 and 5 can also be fitted to the measured data using $\sigma$ as a fitting parameter to obtain $\sigma_{CC}$ and $\sigma_{TOS}$ as the values of interfacial tension obtained by the CC and TOS methods, respectively. A comparison of these values with $\sigma_{eq}$ quantifies the success of either model. Results at all viscosity and aspect ratios are presented in Table 2.

Figure 2 presents retraction data at $L_0/R_0 \approx 8$ in the format suggested by the CC model. The solid lines represent eq 2 with $\sigma = \sigma_{eq}$. It is clear that the lines capture the retraction kinetics very well at low viscosity ratio, but very poorly for $p$ exceeding 1. Fitting eq 2 to the data using $\sigma$ as the fitting parameter, results in $\sigma_{CC}$ values that are close to $\sigma_{eq}$ at low $p$ but much larger than $\sigma_{eq}$ at high $p$ (Table 2). We reiterate that when performing fits, the "linear" region of these plots must be defined somewhat arbitrarily, and significant error may result from improper fitting. Indeed, Demarquette et al.[13] recently reported an unexpectedly high $\sigma_{CC}$ value even for a sample at $p = 0.06$; this may perhaps be related to fitting in an unsuitable region. The conclusion then is that (**1**) $\sigma_{CC}$ will necessarily be much larger than $\sigma_{eq}$ at high $p$ and (**2**) $\sigma_{CC}$ may approach $\sigma_{eq}$ at low $p$, provided the appropriate range of data are chosen for fitting.

Figure 3 replots the same results in the format suggested by the TOS model. The solid lines are eq 5 with $\sigma = \sigma_{eq}$. Clearly, the lines track the data reasonably well at all viscosity ratios. Fitting eq 5 to the data with $\sigma$ as a fitting parameter results in $\sigma_{TOS}$ values that are comparable to $\sigma_{eq}$ at all $p$. The most significant deviations (up to 24%) appear at the smallest aspect ratios; these are at the limit of the expected experimental errors discussed in the previous sections. At lower aspect ratios than those presented here, even larger errors were evident. The conclusion then is that the TOS model yields interfacial tension values close to the equilibrium interfacial tension. Furthermore, while the fits were performed using a linear least-squares analysis, nearly identical values were obtained by "eyeballed" fits, suggesting that the procedure is robust and easy to implement.

In summary, the CC model can give interfacial tension values close to the equilibrium value only at low viscosity ratios. In contrast the TOS model can give interfacial tension values in agreement with the equilibrium value at all viscosity ratios. We believe that the CC model fails at high viscosity ratios because the model is only approximate. In particular, eq 2 was derived from a heuristic argument ($dL/dt$ is proportional to $-dA/$

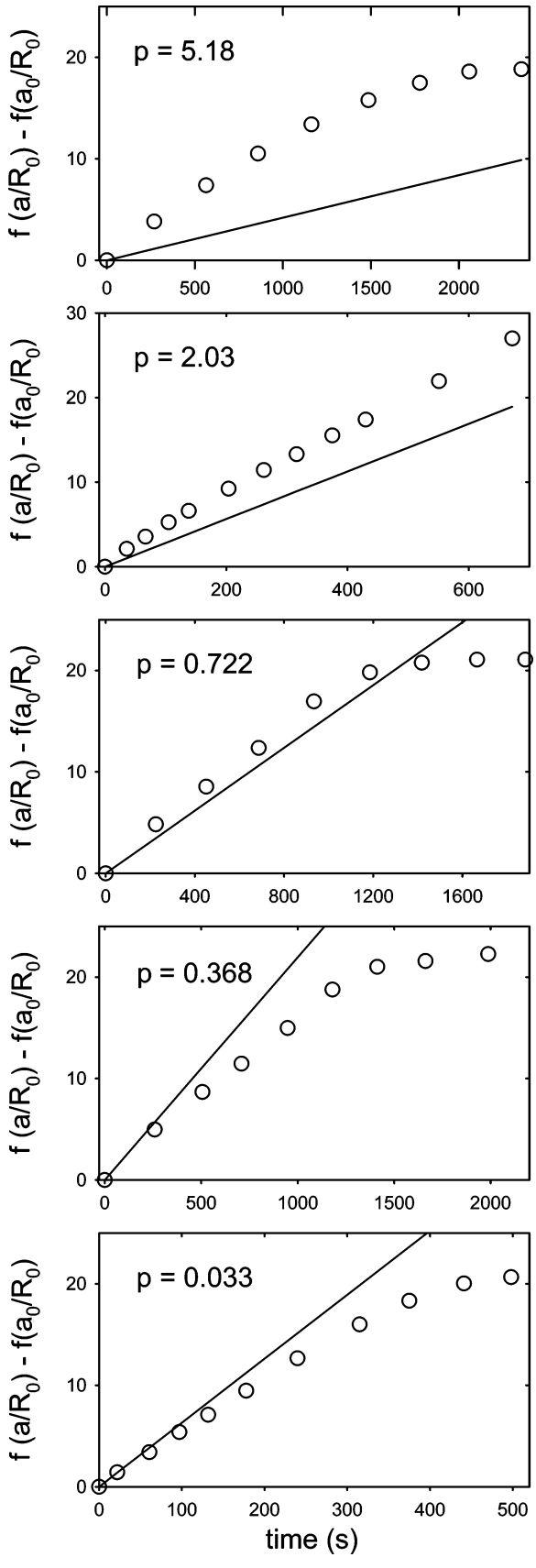


**Figure 2.** Fiber retraction results plotted in the form required by the CC model. Solid lines are eq 2 with $\sigma$ being the equilibrium interfacial tension $\sigma_{eq}$ listed in Table 2.

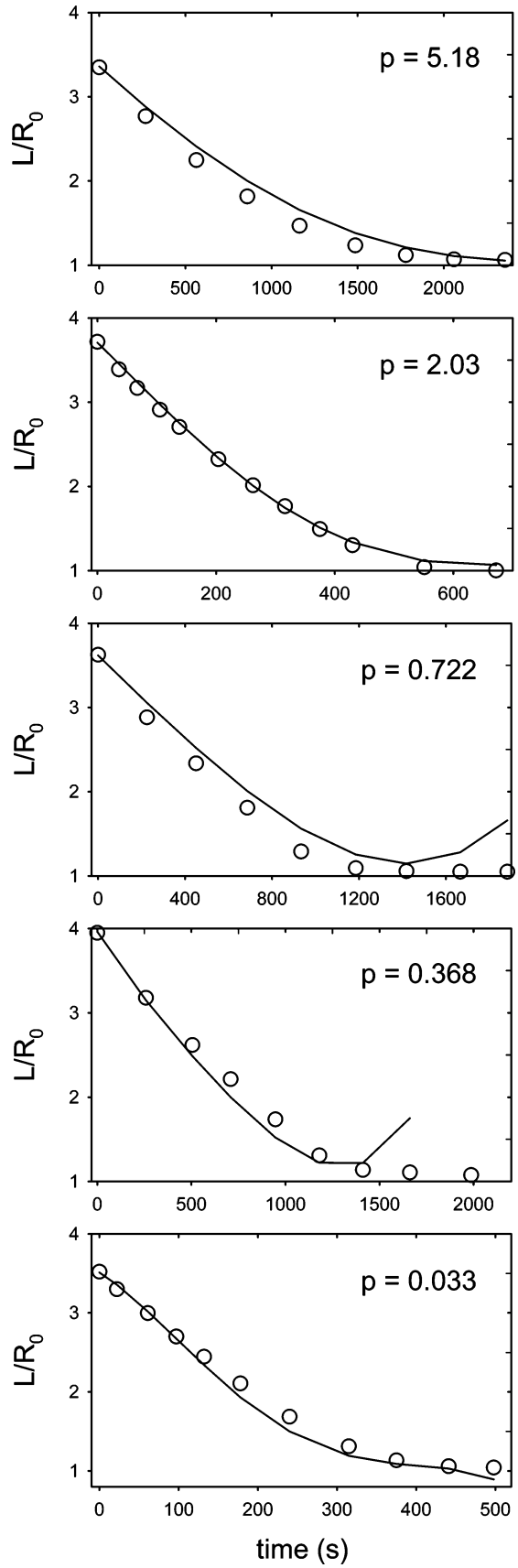


**Figure 3.** Fiber retraction results plotted in the form required by the TOS model. Solid lines are eq 5 with $\sigma$ being the equilibrium interfacial tension $\sigma_{eq}$ listed in Table 2. The upturns in the solid lines at $p = 0.368$ and 0.722 are artifacts of the fourth-order polynomial approximation of the TOS model.

d$L$, where $A$ is the interfacial area of the fiber). Furthermore, the fiber was assumed to be spherocylin-

drical at all times; certainly a questionable approximation for dumbbell shapes. Finally, and perhaps most importantly, eq 4 is a semiempirical approximation of the effective viscosity that was based on parameter fits of a few data sets.[1,2] It may be possible to propose an alternative dependence for $\mu_e$ on $p$ so that the CC method works well at all viscosity ratios. However, rather than such an empirical fix to the CC model, we strongly recommend using the TOS method instead: apart from being reliable and theoretically rigorous, it is also easier to apply than the CC method because (**1**) $a(t)$ does not have to be calculated from eq 1, and (**2**) the fits of eq 5 to the $L/R_0$ vs $t$ data can be done accurately even by visual observation rather than least-squares fits. Indeed we are puzzled that while the TOS model was proposed in 1993, most fiber retraction experiments are still analyzed by the CC model. In fact, a review article on interfacial tension measurements of polymers in 2000[3] even cited a section on capillary instabilities in Tjahjadi et al.,[7] but nevertheless ignored the section on fiber retraction analysis in the same paper. Instead, these reviewers still illustrated the CC model as the only means of analyzing of fiber retraction. A later review[13] and article[14] by Demarquette et al. did state that the CC model gave higher interfacial tensions than the TOS model but did not evaluate the effects of viscosity ratio or aspect ratio of the fibers. Finally, Zeigler and Wolf[15] have also commented that interfacial tensions by the CC method seem to be at variance with that from elliospidal drop retraction analyses, but no comparisons with the equilibrium interfacial tension or with the TOS analysis were made.

## 5. Summary and Conclusions

Two alternate methods of analysis of the imbedded fiber retraction technique for measuring the interfacial tension between molten polymers are evaluated. Experiments were conducted using Newtonian polymer melts and the ratio of the fiber viscosity to the matrix viscosity ranged from roughly 0.03 to 5. Retraction of fibers of aspect ratios ranging from 3 to 14 were studied and the equilibrium interfacial tension was measured independently in the same experiments. The Tjahjadi, Ottino, and Stone analysis[7] gave reliable interfacial tension values at all viscosity ratios; however, initial aspect ratios of less than 3 gave significant errors in the interfacial tension. The analyses of Cohen and Carriere[1,2] gave accurate interfacial tension values at low viscosity ratios but greatly overestimated the interfacial tension at high viscosity ratios. We recommend that the more rigorous and easier-to-use method of Tjahjadi, Ottino, and Stone be used for analyzing fiber retraction data.

**Acknowledgment.** We are grateful to Rhodia Silicones and Soltex Chemicals for providing the experimental materials and the donors of the Petroleum Research Fund, administered by the American Chemical Society (Grant #39931-G9), for sponsoring this research.

## References and Notes

(1) Carriere, C. J.; Cohen, A.; Arends, C. B. *J. Rheol.* **1989**, *33*, 681.
(2) Cohen, A.; Carriere, C. J. *Rheol. Acta* **1989**, *28*, 223.
(3) Xing, P. X.; Bousmina, M.; Rodrigue, D.; Kamal, M. R. *Macromolecules* **2000**, *33*, 8020.
(4) Gramespacher, H.; Meissner, J. *J. Rheol.* **1992**, *41*, 27.
(5) Elemans, P. H. M.; Janssen, J. M. H.; Meijer, H. E. H. *J. Rheol.* **1990**, *34*, 1311.
(6) Luciani, A.; Champagne, M. F.; Utracki, L. A. *J. Polym. Sci., Polym. Phys. Ed.* **1997**, 1393.
(7) Tjahjadi, M.; Ottino, J. M.; Stone, H. A. *AIChE J.* **1994**, *40*, 385.
(8) Stone, H. A.; Leal, L. G. *J. Fluid Mech.* **1989**, *198*, 399.
(9) Vonnegut, B. *Rev. Sci. Instrum.* **1942**, *13*, 6.
(10) Princen, H. M.; Zia, I. Y. Z.; Mason, S. G. *J. Colloid Interface Sci.* **1967**, *23*, 99.
(11) Joseph, D. D.; Arney, M. S.; Gillberg, G.; Hu, H.; Hultman, D.; Verdier, C.; Vinagre, T. M. *J. Rheol.* **1992**, *36*, 621.
(12) Puig, J. E.; Seeto, Y.; Pesheck, C. V.; Scriven, L. E. *J. Colloid Interface Sci.* **1992**, *148*, 459.
(13) Demarquette, N. R.; De Souza, A. M. C.; Palmer, G.; Macaubas, P. H. P. *Polym. Eng. Sci.* **2003**, *43*, 670.
(14) Palmer, G.; Demarquette, N. R *Polymer* **2005**, *46*, 8169.
(15) Zeigler, V. E.; Wolf, B. A. *Langmuir* **2004**, *20*, 8688.

MA050509K